



Effect of aridification on carbon isotopic variation and ecologic evolution at 5.3 Ma in the Asian interior

Jimin Sun ^{a,*}, Tongyan Lü ^b, Yingzeng Gong ^a, Weiguo Liu ^c, Xu Wang ^a, Zhijun Gong ^a

^a State Key Laboratory of Lithospheric Evolution, Institute of Geology and Geophysics, Chinese Academy of Sciences, PO Box 9825, Beijing 100029, China

^b Institute of Geomechanics, Chinese Academy of Geological Sciences, Beijing, China

^c Institute of Earth Environment, Chinese Academy of Sciences, Xi'an 710075, China



ARTICLE INFO

Article history:

Received 12 April 2012

Received in revised form 31 July 2013

Accepted 13 August 2013

Available online 31 August 2013

Editor: G. Henderson

Keywords:

stable carbon isotope

latest Miocene

C₄ expansion

Asian interior

ABSTRACT

The Cenozoic era is marked by dramatic climatic and ecological changes. The timing of the emergence and the subsequent expansions of C₄ grasses are prominent biological events on Earth. In China, thick Cenozoic deposits in the Tarim and Junggar Basins, which are located in the Asian interior, provide important geological archives for studying paleoenvironmental changes. Here we use carbon isotope compositions of organic matter to reconstruct the history of ecologic evolution during the late Cenozoic in the Tarim and Junggar Basins. The results show that there is a shift to slightly higher $\delta^{13}\text{C}$ values at 5.3 Ma indicating a change in terrestrial ecosystems in the Asian interior driven by an increased regional aridity rather than decreasing atmospheric $p\text{CO}_2$ levels. The weakened water vapor transportation related to the retreat of Paratethys Ocean and the enhanced rain shadow effect of mountain uplift during the latest Miocene mostly triggered this event.

© 2013 Elsevier B.V. All rights reserved.

1. Introduction

The Cenozoic world climate has prominent stepwise cooling and drying trends, marked by the initiation of ice sheet in the Antarctic since the Eocene–Oligocene boundary at 34 Ma (e.g., Kennett, 1977; Miller et al., 1991; Zachos et al., 2001) and the emergence of high latitude sea ice in the northern hemisphere in the late Cenozoic at about 7–5 Ma (e.g., Jansen and Sjøholm, 1991; Larsen et al., 1994). Over the same time span, grasslands expanded in terrestrial ecosystems (Jacobs et al., 1999). Although the emergence of C₄ plants on earth may be as early as 32 to 23 Ma (e.g., Fox and Koch, 2003; Osborne and Beerling, 2006; Urban et al., 2010; Edwards et al., 2010), the significant C₄ expansion occurred much later, mostly from the latest Miocene to Pliocene or even into the Pleistocene (e.g., Quade et al., 1989; Cerling et al., 1993, 1997; Dettman et al., 2001; Retallack, 2001; Bywater-Reyes et al., 2010; Fox et al., 2012a, 2012b).

However, there have been different opinions about the causes of C₄ expansion in the late Neogene. Quade et al. (1989) linked the dramatic ecologic shift in the latest Miocene in Pakistan to a marked strengthening of the Asian monsoon system. Cerling et al. (1997) proposed that a drop in atmospheric CO₂ levels drove this expansion, but the later established CO₂ record indicates more or less steady levels throughout the Neogene (e.g., Pagani et al., 2005).

Pagani et al. (1999) attributed the C₄ plant expansion to enhanced regional aridity or changes in seasonal precipitation patterns. Other alternative views include that grasslands were a biological force in their own right (Retallack, 1998) or the worldwide rapid increase in C₄ ecosystem responded to both climate and tectonics (Kohn and Fremd, 2008).

Not only the causes for the late Miocene C₄ expansions are controversial, but also the exact timing of this ecological event is still debated. Quade et al. (1989) reported dramatic ecological shift beginning ~7.4–7.0 Ma in Pakistan. Cerling et al. (1993) concluded that C₄ expansions occurred between 7 and 5 Ma in Pakistan and North America, and later Cerling et al. (1997) suggested a global scale C₄ expansion at 8–6 Ma. Latorre et al. (1997) suggested that the presence of C₄ plants started at 7.3–6.7 Ma in Argentina. Fox and Koch (2004) indicated that the percentage of C₄ grasses in the Great Plains of the United States increased from 6.4 to 4.0 Ma; later, more records in the central Great Plains indicate C₄ expansion from the early late Miocene to the early Pleistocene (e.g., Martin et al., 2008; Fox et al., 2012a, 2012b). Additionally, $\delta^{13}\text{C}$ values of *n*-alkanes from the Gulf of Mexico indicate that terrigenous C₄ plants steadily increased during the late Miocene into the Pleistocene (Tipple and Pagani, 2010). The recent higher-resolution study on the well-known Siwalik Group of Pakistan revealed a more gradual transition between 8.0 and 4.5 Ma in which C₃ and C₄ plants occupied different subenvironments of the Siwalik alluvial plain (Behrensmeyer et al., 2007). In South Africa, C₄ grasses became a significant part of the Makapansgat Valley ecosystem at approximately 4–5 Ma (Hopley et al.,

* Corresponding author. Tel.: +86 10 8299 8389.

E-mail address: jmsun@mail.igcas.ac.cn (J. Sun).

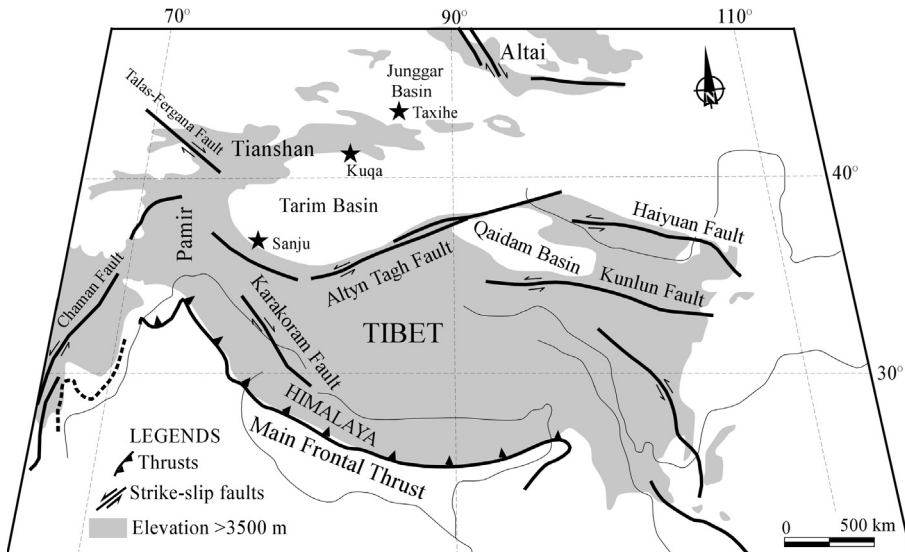


Fig. 1. Simplified geological map shows the main active faults of central Asia as well as the locations (black stars) of the sections mentioned in the text (modified from Avouac and Tapponnier, 1993).

2007). In central North China, Ding and Yang (2000) defined a major expansion of C₄ plants at ca. 4.0 Ma. Wang and Deng (2005) and Biasatti et al. (2010) presented extensive isotope data and suggested that C₄ grasses were either absent or insignificant in the Linxia Basin prior to ~2–3 Ma and only became a significant component of local ecosystems in the Quaternary. Significant C₄ biomass was also reported in the Gyirong Basin in southern Tibet at ~7 Ma (Wang et al., 2006) and in the central Inner Mongolia from ~8 to 4 Ma (Zhang et al., 2009). In South China Sea, the δ¹³C record of black carbon of marine sediments indicates an increasing trend since 8.7 Ma (Jia et al., 2003).

The C₄ expansion can be studied by using carbon isotopic compositions of sediments. Previous studies have demonstrated that the C₃ and C₄ photosynthetic pathways fractionate carbon isotopes to different degrees; C₃ and C₄ plants have averaged δ¹³C values of −27‰ and −13‰, respectively (Cerling et al., 1997). Different from the soil carbonate and mammalian fossil tooth enamel which are significantly enriched in δ¹³C compared to source carbon, organic matter preserves the isotopic distinction with little or no isotopic fractionation (Cerling et al., 1989).

In China, huge inland basins occupy northwestern China. The remote distances to oceans (both the Pacific and the Atlantic oceans) make this region the driest region in the interior of Asia. To date, there are only limited carbon isotope records available from this region (e.g., Wang and Deng, 2005; Charreau et al., 2012; Zhang et al., 2009, 2012). In this paper, we report the results of stable carbon isotope analyses of organic matter in order to discuss the timing and driving mechanisms of significant late Cenozoic ecological changes in the interior of Asia.

2. Geological setting

The Asian interior consists of several east–west trending mountain ranges (e.g., Kunlun Mountains, Tianshan Mountains), forming a series of mountain–basin systems. In this paper, we focus on studying the past ecological changes in the Tarim and Junggar Basins (Fig. 1). The Tarim Basin is the largest inland basin in China and is constrained by three large mountain ranges: the Tianshan range to the north, the Pamir Mountain to the west, and the Kunlun range to the south (Fig. 1). Located in the rain shadow of the Tibetan Plateau, the climate is extremely dry with annual rainfall of less than 50 mm in the center of the basin, and it is the driest

region in the interior of Asia. The main part of the basin is occupied by the Taklimakan Desert, which covers an area of 132,000 square miles (342,000 km²) and is the world second largest shifting sand desert on Earth (Zhu et al., 1980).

The Junggar Basin is constrained by the Altay Mountains to the northeast and the Tianshan Mountains to the south (Fig. 1). This basin has an area of 380,000 km² and the center of the basin is the Gurbantunggut Desert. The annual precipitation ranges from 70 to 250 mm and it is a steppe and semi-desert basin.

Both basins are of structural origins. The Cenozoic uplifts of the surrounding mountains are related to the continuing convergence of India and Eurasia since their collision in the Eocene (Molnar and Tapponnier, 1975). Being coupled with the mountain uplift, both basins experienced major subsidence during the Cenozoic era. The Cenozoic sedimentary rocks derived from the surrounding mountain belts accumulated in the foreland basins with a thickness of up to 10 km (e.g., Li et al., 1996; Jia, 1997). The tectonically deformed Cenozoic sediments not only provide useful constraints on the mountain building in the surrounding orogens but also serve as an important archive for studying past ecological evolution.

In this study, two sections were chosen for studying paleovegetation changes. Among them, the Sanju (37°11'N, 78°29'E) section lies in the southern edge of the Tarim Basin (Fig. 1), while the Taxihe section (44°06'N, 86°20'E) is located in the southern margin of the Junggar Basin (Fig. 1).

The strata of the above sections are all tectonically deformed by thrusting and folding in the foreland basins (Fig. 2). The studied deposits at Sanju span an age range from late Miocene to Quaternary (Sun and Liu, 2006), with a thickness of 1626 m, and consist of the late Miocene Pakabulake Formation, the Pliocene Artux Formation, and the latest Pliocene to early Pleistocene Xiyu Formation (Fig. 2a).

The Taxihe section is an overturned anticline, with steep or overturned strata in the core of the northern limb and a gently dipping southern limb (Fig. 2b), consisting of the Oligocene Anjihahe Formation (E3a), the latest Oligocene Shawan Formation (E3s), the Miocene Taxihe Formation (N1t), the Pliocene Dushanzi Formation (N2d), and the early Pleistocene Xiyu (Q1x) Formation (Fig. 2b). The Taxihe section is 2960 m thick (Sun and Zhang, 2009). Generally, there is an up section trend towards coarser grain size from the late Oligocene Shawan to the early Pleistocene Xiyu Formations.

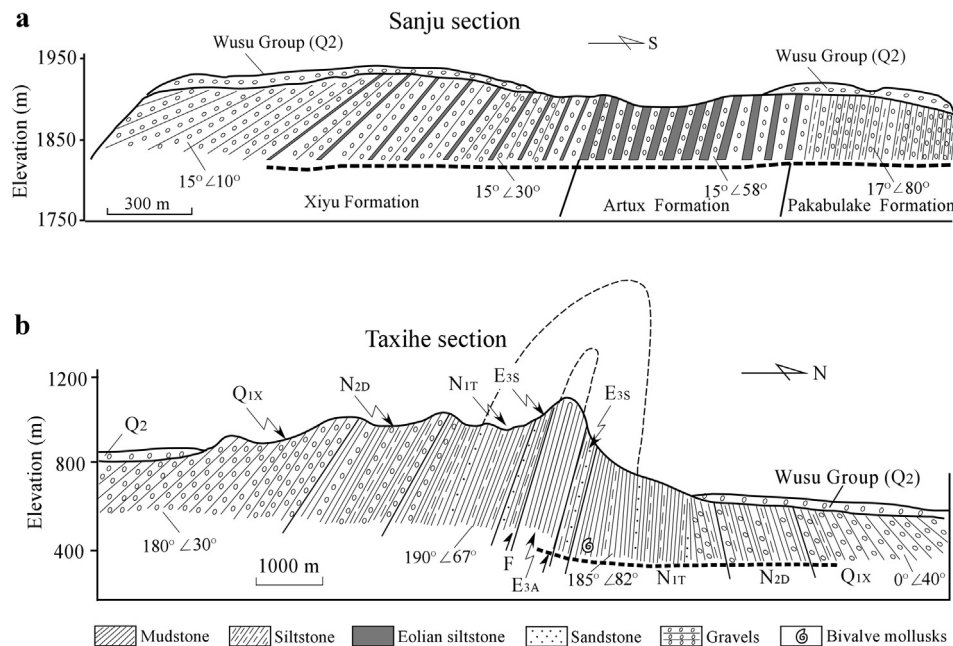


Fig. 2. Cenozoic strata of the two sections chosen for stable carbon isotope analysis within the Tarim and Junggar Basins, (a) the Sanju section, and (b) the Taxihe section. The bold dashed lines indicate our sampling routes. E3a: Oligocene Anjihaihe Formation; E3s: Late Oligocene Shawan Formation; N1t: Miocene Taxihe Formation; N2d: Pliocene Dushanzi Formation; Q1x: Early Pleistocene Xiyu Formation; Q2: Middle Pleistocene; F: Thrust Fault.

EPOCH	DEPTH (m)	LITHOLOGY	MPTS Ma	TEXTURE	SEDIMENTARY FACIES
Pleistocene (Xiyu Fm.)	0			Thick dark grey conglomerates with interbedded thin light-yellow siltstone	Proluvial fan with eolian silt accumulation
	100				
	200		2.58		
Pliocene (Artux Fm.)	300				
	400				
	500				
	600				
	700		3.58	Alternations of dark grey conglomerates and light-yellow siltstone	Alluvial and flood fan with episodically eolian silt accumulation
	800				
	900				
	1000		5.3		
Miocene (Pakabulake Fm.)	1100				
	1200				
	1300				
	1400				
	1500				
	1600		6.5	Alternations of dark grey conglomerates and brownish to reddish siltstone	Fluvial channel fan and floodplain
		Conglomerate	Alluvial siltstone	Wind-blown siltstone	

Fig. 3. Lithology and sedimentary facies of the Sanju section in the southern Tarim Basin.

3. Sedimentary facies and age assignment

For the Sanju section, the sedimentary record is characterized by continental deposits (Fig. 3). The late Miocene Pakabulake Formation is characterized by alternations of dark grey conglomerates

and brownish to reddish siltstone, implying sedimentary facies of fluvial channel fan and flood plain. The Pliocene Artux Formation consists of dark grey conglomerates and light-yellow siltstone, representing sedimentary facies of alluvial and flood fan with episodically eolian silt accumulation. The latest Pliocene to early

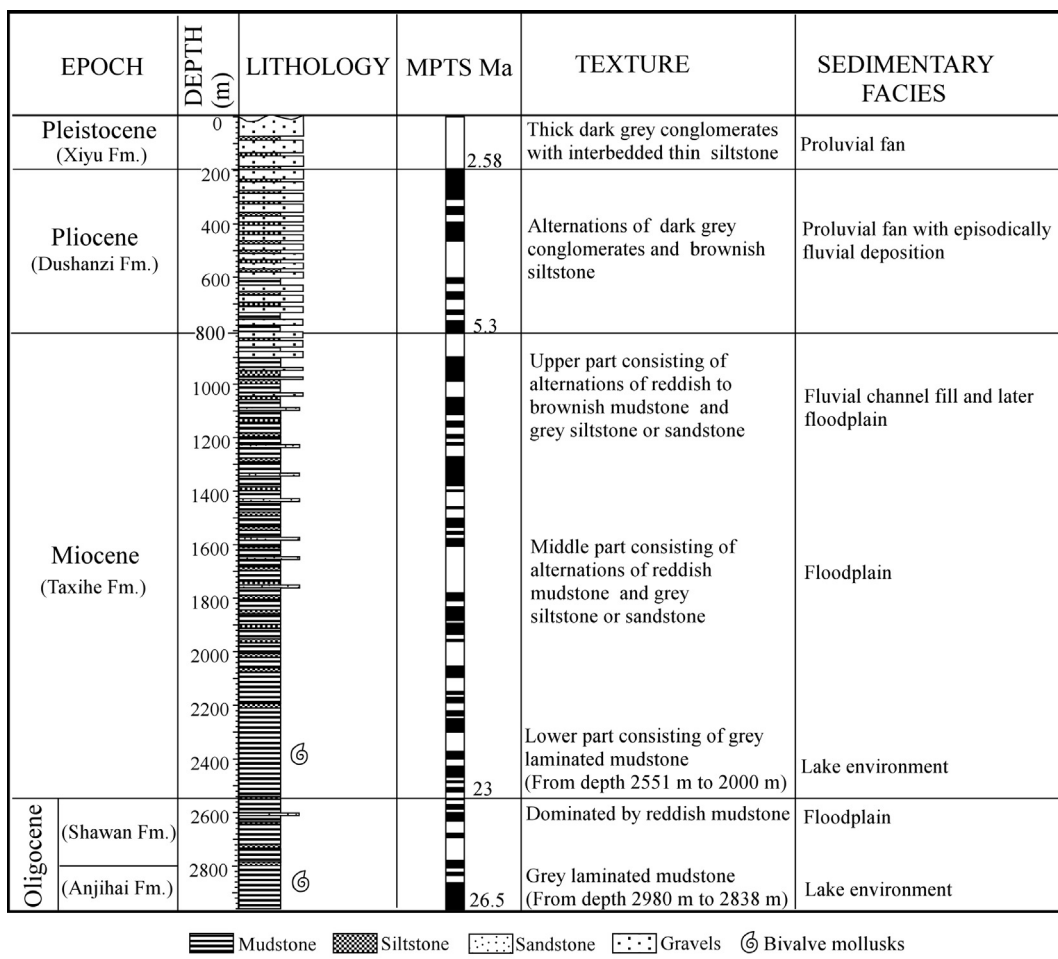


Fig. 4. Lithology and sedimentary facies of the Taxihe section in the southern Junggar Basin.

Pleistocene Xiyu Formation is dominated by dark grey conglomerates with thin light-yellow siltstone intercalations, representing sedimentary environment of proluvial fan and occasionally eolian deposition.

Age assignments of the Sanju section are obtained by correlating the measured magnetic polarity (Sun and Liu, 2006) to the paleomagnetic time scale of Cande and Kent (1995) from C3An.2n to C2r.1n, yielding an age range of ca. 6.5 to ~2.0 Ma (Sun and Liu, 2006).

The sedimentary facies of the Taxihe section are quite diverse (Fig. 4). The oldest stratum is the Oligocene Anjihaihe Formation, and it is typical grey lacustrine mudstone. The latest Oligocene Shawan Formation is dominated by reddish mudstone with occasionally sandstone or fine gravel intercalations representing sedimentary facies of floodplain. The Miocene Taxihe Formation can be subdivided into three parts: the lower part of grey lacustrine mudstone; the middle part of alternations of reddish mudstone and grey siltstone or sandstone; and the upper part of alternations of reddish to brownish mudstone and grey siltstone or sandstone. The Pliocene Dushanzi Formation consists of alternations of dark grey conglomerates and brownish siltstone, indicating environment of proluvial fan with episodically fluvial deposition. The uppermost part is the Xiyu Formation dominated by dark grey pebble to boulder conglomerates, being proluvial fan environment.

Age assignments of the Taxihe section are based on biostratigraphic age controls and paleomagnetic polarity correlations, suggesting an age range of 26.5 to 2.58 Ma (Sun and Zhang, 2009).

4. Sampling and methods

In this study, a total of 325 bulk sediment samples were collected for organic matter carbon isotope analysis. Among them, 144 and 181 samples were taken from the Sanju and the Taxihe sections, respectively.

Samples for organic matter carbon stable isotope analysis were first screened for modern rootlets and then digested for at least 15 h in 1 M HCl to remove inorganic carbonate. The samples were then washed with distilled water and dried. The dried samples (~480 mg) were combusted for over 4 h at 900 °C in evacuated sealed quartz tubes in the presence of 0.5 g Cu, 4.5 g CuO and 0.2 g Ag foil. The CO₂ was purified and isolated by cryogenic distillation for isotopic analysis. The isotopic composition of CO₂ was then measured using a Finnigan MAT 253 mass spectrometer. The analyses are calibrated using the external working standard Glycine ($\delta^{13}\text{C}_{\text{VPDB}} = -33.30\text{\textperthousand}$), which is repeatedly calibrated using the international standard USGS 24 (graphite). The carbon isotope results are expressed in conventional delta (δ) notation as the per mil (‰) deviation from the standard Peedee belemnite (PDB). For the sequential measurement on the OM samples, the external working standard materials were inserted between every 6 samples to monitor the working conditions of the analyzer. The precision for analysis of the external standard was better than ±0.1‰. Recurrent analyses ($n = 9$) of sample show that this procedure yields a precision better than ±0.2‰.

In order to evaluate the equality of means of $\delta^{13}\text{C}$ data, statistical tests (Levene's test and *t*-test) were done using PASW statistics

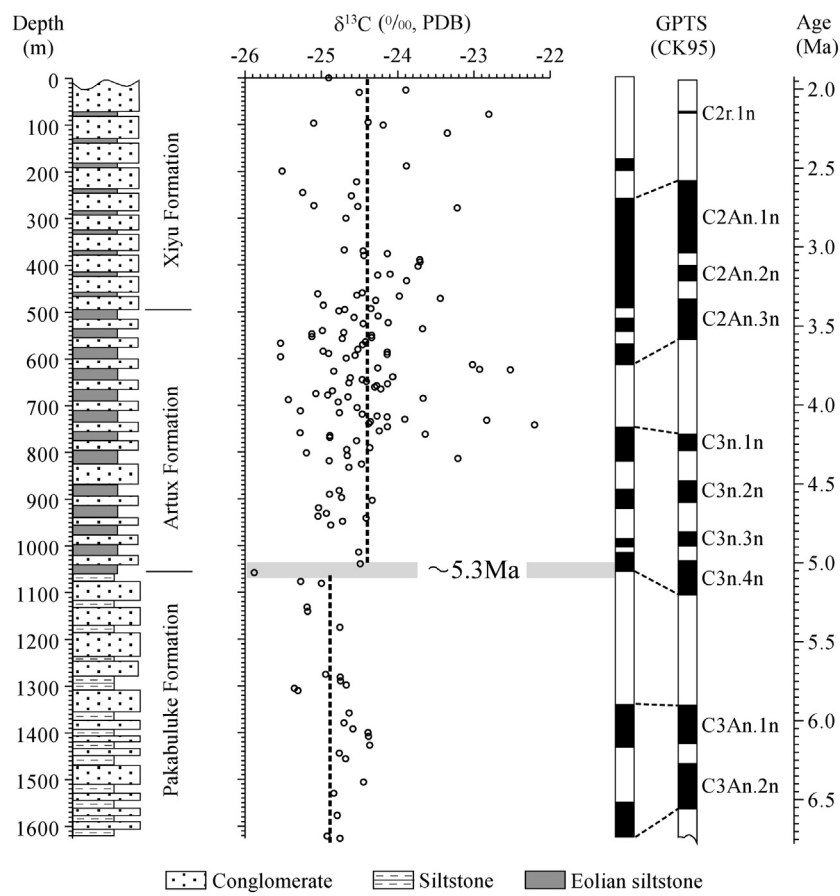


Fig. 5. Vertical variations of organic matter $\delta^{13}\text{C}$ of the Sanju section in the southern Tarim Basin. Dash lines represent the average $\delta^{13}\text{C}$ values. Magnetic polarity age control is from Sun and Liu (2006).

18 (formerly SPSS statistics). The $\alpha = 0.05$ criterion was used to evaluate the statistical significance of the tests.

5. Results

5.1. Variations of $\delta^{13}\text{C}$ values in the southern margin of the Tarim Basin

The carbon isotopic values of organic matter versus depth at Sanju are shown in Table A.1 and Fig. 5. The $\delta^{13}\text{C}$ values of the organic matter at Sanju range from $-25.9\text{\textperthousand}$ to $-22.2\text{\textperthousand}$ and average $-24.5\text{\textperthousand} \pm 0.6\text{\textperthousand}$. Examination of the carbon isotope records indicates that there is a shift to higher $\delta^{13}\text{C}$ values at ~ 5.3 Ma. The averaged $\delta^{13}\text{C}$ value of organic matter is $-24.85\text{\textperthousand} \pm 0.36\text{\textperthousand}$ ($n = 25$) from 6.5 to 5.3 Ma, and it increases to $-24.42\text{\textperthousand} \pm 0.61\text{\textperthousand}$ ($n = 119$) after 5.3 Ma (Fig. 5). The means for $\delta^{13}\text{C}$ values before and after 5.3 Ma are distinguishable on the basis of a Levene's test and a two-tailed t -test assuming unequal variances (Table 1). Levene's test significance statistic is 0.046; t -test significance is 1.3×10^{-5} ; all p values based on $\alpha = 0.05$.

5.2. Long-term variations of $\delta^{13}\text{C}$ values in the southern Junggar Basin

The long-term carbon isotopic values in the Taxihe section are shown in Table A.2 and Fig. 6. The $\delta^{13}\text{C}$ values of organic matter at Taxihe fall between $-26.7\text{\textperthousand}$ and $-18.4\text{\textperthousand}$, with an average value $-22.6 \pm 1.3\text{\textperthousand}$. The averaged $\delta^{13}\text{C}$ value of organic matter is $-22.84\text{\textperthousand} \pm 1.21\text{\textperthousand}$ ($n = 131$) from 26.5 to 5.3 Ma, and it increases to $-21.85\text{\textperthousand} \pm 1.24\text{\textperthousand}$ ($n = 50$) after 5.3 Ma (Fig. 6). This fluctuation curve shows a shift to slightly higher $\delta^{13}\text{C}$ values after ~ 5.3 Ma. Although the Levene's test significance statistic is 0.945, the t -test significance use the “Equal variances assumed” is less than 0.001.

(Table 1), suggesting different means of $\delta^{13}\text{C}$ values before and after 5.3 Ma.

It is important to stress that there are lacustrine mudstone spanning 2960–2800 m and 2500–2275 m, corresponding to age ranges of 26.5–25.2 Ma and 22.8–20.2 Ma, respectively (Fig. 6). Because lacustrine organic matter can be isotopically light (e.g., Meyers and Horie, 1993; Liu et al., 2013), the $\delta^{13}\text{C}$ values are as low as $-26.7\text{\textperthousand}$ in such lacustrine mudstone can be mostly explained by the different carbon isotope compositions between lacustrine organic matter and terrestrial samples.

6. Discussions

The long-term variations of $\delta^{13}\text{C}$ values of the two sections all show a shift to higher values beginning at about 5.3 Ma. Here, we present alternative interpretations for the stable carbon isotope fluctuations.

6.1. Factors influencing the $\delta^{13}\text{C}$ shift at ~ 5.3 Ma in the Asian interior

Modern plants fall into three groups, based on their photosynthetic pathways: C₃, C₄, and CAM. Plants exhibiting C₃ photosynthesis have dominated the history of terrestrial vegetation; C₄ plants became abundant in grasslands only in the late Cenozoic (Cerling et al., 1997; Edwards et al., 2010). CAM plants occupy only a small percentage of typical ecosystems. These three groups of plants have different carbon isotope compositions, C₃ plants exhibit a large range varying from $-37\text{\textperthousand}$ to $-20\text{\textperthousand}$ (Kohn, 2010), C₄ plants have $\delta^{13}\text{C}$ values ranging from $-16\text{\textperthousand}$ to $-10\text{\textperthousand}$, while the $\delta^{13}\text{C}$ values of CAM plants typically range from $-20\text{\textperthousand}$ to $-10\text{\textperthousand}$ (O'Leary, 1988).

Table 1

Results of the *t*-test analysis of the organic $\delta^{13}\text{C}$ data before and after 5.3 Ma.

Sections	Hypothesis	Levene's test for equality of variances		<i>t</i> -test for equality of means					95% confidence interval of the difference	
		F	Sig.	<i>t</i>	df	Sig. (2-tailed)	Mean difference	Std. error difference		
Sanju	Equal variances assumed	4.064	0.046	-3.397	142	0.001	-0.4320	0.1272	-0.6834	-0.1806
	Equal variances not assumed			-4.763	58.68	0.000	-0.4320	0.0907	-0.6136	-0.2505
Taxihe	Equal variances assumed	0.005	0.945	4.874	179	0.000	0.9864	0.2024	0.5870	1.3858
	Equal variances not assumed			4.829	87.07	0.000	0.9864	0.2043	0.5804	1.3924

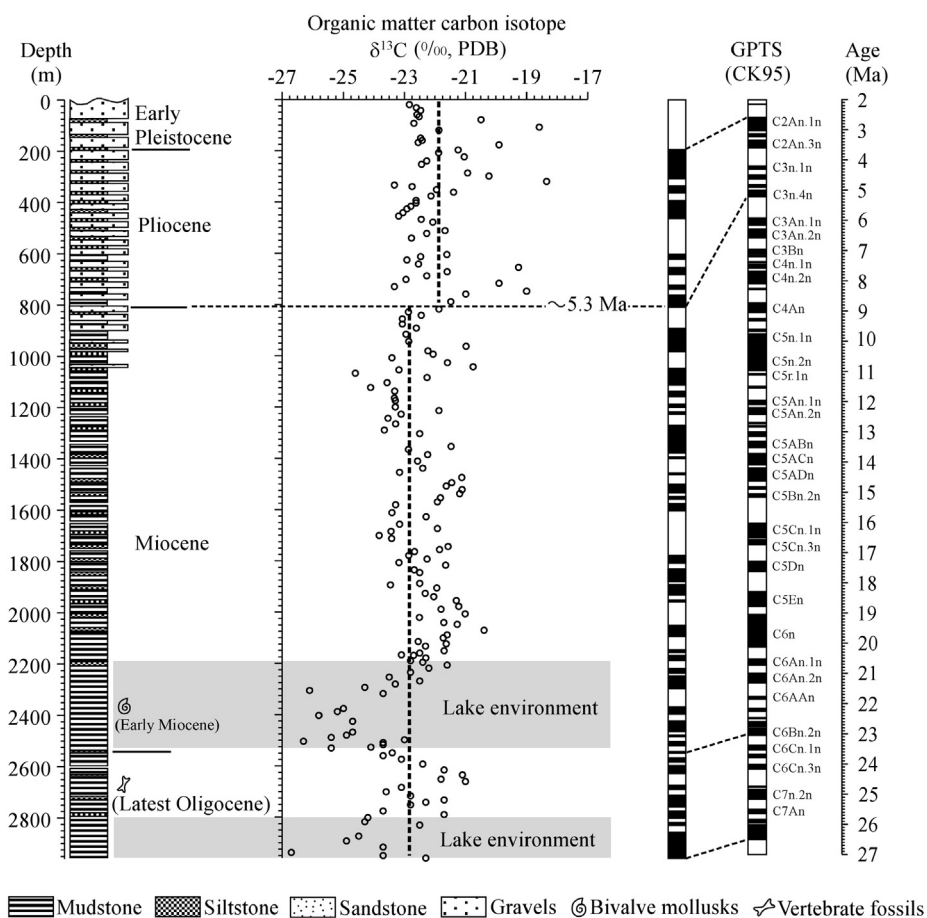


Fig. 6. Variations of organic matter $\delta^{13}\text{C}$ versus depth of the Taxihe section in the southern Junggar Basin. Dash lines represent the average $\delta^{13}\text{C}$ values. Magnetic polarity time scale is from Sun and Zhang (2009).

Although changes in vegetation types can consequently impact the sedimentary organic carbon isotopic compositions, a variety of environmental factors also influence the carbon isotopic composition of organic matter (O'Leary, 1981; Meyers, 1992; Stevenson et al., 2005). These include the concentration and the $\delta^{13}\text{C}$ of atmospheric CO_2 , carbon source, temperature, light intensity, and water stress.

Carbon isotopic variations are associated with fluctuations in atmospheric CO_2 content. Under conditions of increased CO_2 , C_3 photosynthesis is more efficient than C_4 or CAM photosynthesis (Cerling et al., 1993). The carbon isotope ratio of plant material also depends on the $\delta^{13}\text{C}$ of atmospheric CO_2 , which likely varied throughout Earth history (Tipple et al., 2010). It is well known that the $\delta^{13}\text{C}$ values of atmospheric CO_2 and plants have become 1.5‰

more negative since the industrial revolution (Tipple et al., 2010), due to inputs of ^{13}C -depleted CO_2 from burning of fossil fuels.

The isotopic composition of the carbon source can also affect the $\delta^{13}\text{C}$ values. The carbon isotopic compositions of various aquatic plants are often different from terrestrial plants, and recycling of isotopically light land-derived organic carbon in coastal marine and lacustrine waters can create an isotopic shift to lighter values in algal organic matter (Meyers and Horie, 1993).

Photosynthesis under high light and temperature is crucial for the ecological dominance of C_4 plants due to their higher photosynthetic efficiency (Osmond et al., 1982; Long, 1999). Under a range of light conditions, from light-limited to light-saturated (e.g., a dense or open grass canopy), carbon assimilation should

be greater for C₄ grasses compared with C₃ grasses at higher temperatures, and vice versa at lower temperatures (Still et al., 2003).

Water stress is one of the most limiting environmental factors affecting carbon isotopic composition of plants. Drought stress decreases stomatal conductance, increasing the ratio of external to internal CO₂ partial pressures. As a result, $\delta^{13}\text{C}$ differences of 1–3‰ have been noted in laboratory and field experiments involving a single species grown at various moisture levels (Farquhar and Richards, 1984; Read et al., 1991, 1992). Moreover, C₄ grasses have higher water use efficiency than that of C₃ plants (Raven et al., 1999; Emmerich, 2007). The widespread expansion of C₄ grasses since the late Miocene was driven primarily by their higher water use efficiency, which allowed them to exploit high-light, fire-prone areas in a increasingly seasonal and arid world (Fox and Koch, 2004; Huang et al., 2007).

For the long-term variation $\delta^{13}\text{C}$ record of the two sections, which indicates a shift to higher values beginning at about 5.3 Ma, there are three alternative interpretations: (1) expansion of C₄ grasses in the Asian interior, (2) increase of CAM plants, and (3) changes in C₃ species.

Firstly, C₄ plants have significantly higher $\delta^{13}\text{C}$ values than C₃ plants (Cerling et al., 1997). Thus, the increase in the mean $\delta^{13}\text{C}$ values observed in both sections (Figs. 5 and 6) is probably due to the expansion of C₄ grasses in the Asian interior at ~5.3 Ma. This can be supported by the pollen evidence which indicates that both of the Chenopodiaceae and Gramineae pollen assemblages greatly increased in the two sections since the latest Miocene (Sun et al., 2008; Sun and Zhang, 2008).

Secondly, the $\delta^{13}\text{C}$ values of CAM plants are also generally higher than those of C₃ plants (O'Leary, 1988). In this context, the slightly increase of the averaged $\delta^{13}\text{C}$ values of the two sections beginning at 5.3 Ma may be attributed to the increase of CAM plants. However, both the modern vegetation investigations in the arid basins of northwestern China (Su et al., 2011) and the geological pollen results demonstrate that CAM plants are very rare (e.g., Sun et al., 2008; Zhang and Sun, 2011). Therefore, the relatively higher $\delta^{13}\text{C}$ values beginning at 5.3 Ma could not be interpreted by the expansion of CAM plants.

Finally, the higher $\delta^{13}\text{C}$ values since the latest Miocene can be also explained by the changes of C₃ biomass. It is well known that the $\delta^{13}\text{C}$ values of atmospheric CO₂ and plants have become 1.5‰ more negative since the industrial revolution (e.g., Tipple et al., 2010). In other words, C₃ plants in the pre-industrial times or geologic past had higher $\delta^{13}\text{C}$ values than their modern counterparts. Moreover, compilations of $\delta^{13}\text{C}$ values of both C₃ and C₄ plants exhibit considerable variation in both categories, but particularly in C₃ plants in relation to environmental factors (Diefendorf et al., 2010; Kohn, 2010). Although the average $\delta^{13}\text{C}$ value for modern C₃ plants is −27‰, it is well known that C₃ plants are enriched in ¹³C under water-stressed conditions and can have $\delta^{13}\text{C}$ values as high as −20‰ in arid environments (Diefendorf et al., 2010; Kohn, 2010). In this context, the $\delta^{13}\text{C}$ values reported for the Sanju section and the Taxihe section can also be explained by changes in aridity and/or C₃ species composition.

6.2. Regional aridity driving long-term carbon isotope fluctuation and ecological evolution since the latest Miocene

It is an interesting question why higher $\delta^{13}\text{C}$ values and thus ecological evolution occurred in the interior of Asia since the latest Miocene.

In recent years, the history of aridity in the Tarim Basin has been studied by many authors (e.g., Fang et al., 2002; Zheng et al., 2002, 2003, 2010; Sun and Liu, 2006; Sun et al., 2008, 2009a; Tada et al., 2010; Sun et al., 2011). For the Sanju section, an earlier work mainly using sedimentology method indicates that the

eolian siltstone began to accumulate in the Sanju section at least since 5.3 Ma, suggesting the dune field in the center of the basin (the source of the eolian silt) must have been of considerable size (the embryo of the present Taklimakan Desert) since the Miocene–Pliocene boundary (Sun and Liu, 2006). A later work in the interior of the basin identified *in situ* eolian sand dunes at about 7 Ma (Sun et al., 2009a). The co-existence in the section of eolian sands with lacustrine and fluvial deposits mostly implies widespread extradune environments during this period (Fig. 7a) and limited occurrence of dune fields in the basin interiors (Sun et al., 2009a). However, after 5.3 Ma, a large size dune field existed in the Tarim Basin (Fig. 7b).

The intensified aridity in the Tarim Basin beginning at 5.3 Ma can be also demonstrated by multiple climatic proxies within the basin. In the Sanju section, concentrations of soluble salts (e.g., Cl[−], Na⁺) increased by up to 10³ times since 5.3 Ma. Soluble salt contents have been used widely to reflect past salinity conditions and climatic changes in many parts of the world (Wasson et al., 1984; Last, 1990; Schütt, 2000; Dean and Schwab, 2000; Last and Vance, 2002; Sinha and Raymahashay, 2004) especially in arid regions where strong evaporation favors soluble salt accumulation. In this context, the shift to much higher Cl[−] and Na⁺ concentrations implies much intensified aridity since 5.3 Ma (Sun et al., 2008). At the Kuqa section of the northern Tarim Basin, a drought parameter based on previous pollen results also indicates a prominent increase in aridity since 5.3 Ma (Zhang and Sun, 2011). Therefore, multiple parameters throughout the entire Tarim Basin demonstrate much intensified regional aridity since 5.3 Ma ago. This $\delta^{13}\text{C}$ isotopic shift observed in our studied sections in the Asian interior is approximately synchronous with a prominent shift in the oxygen isotopic record from a paleo-lake basin in central Himalayas (Wang et al., 2012), suggesting a significant change in regional climate in the latest Miocene.

Although the shift to slightly higher $\delta^{13}\text{C}$ values since the end of the Miocene can be explained by either the expansion of C₄ grasses or the changes in C₃ species, both of them are related to enhanced regional aridity. The C₄ photosynthesis improves photosynthetic efficiency and minimizes the water loss in hot, dry environments (Edwards and Walker, 1983). In this context, the possible expansions of C₄ grasses can be explained as a response to enhanced aridity in the Asian interior since 5.3 Ma rather than decreased atmospheric pCO₂ proposed by Cerling et al. (1997), because the long-term atmospheric pCO₂ variation does not show major changes since the end of the Oligocene (Pearson and Palmer, 1999; Pagani et al., 2005, 2009). Moreover, even if the carbon isotope shift can be also explained by shifts in C₃ species rather than C₄ expansion, the enrichment of ¹³C in C₃ plants mostly happen in arid environment.

Our evidence demonstrates that the ecological shift in the Asian interior is a response to increased aridity since the end of the Miocene, it is interesting to discuss causes of the increased aridity.

Although significant permanent ice sheets first appeared near the Eocene/Oligocene boundary (~34 Ma) on Antarctica (Kennett, 1977), the temperature record from the magnesium/calcium ratio (Mg/Ca) in benthic foraminiferal calcite of deep-sea sediments indicates that the most dramatic decrease of temperature began ca. 5.3 Ma (Lear et al., 2000, Fig. 8a), and this is mirrored by the remarkable increase of benthic foraminiferal oxygen isotope values (Zachos et al., 2001; Fig. 8b), which is mostly related to global ice volume changes (e.g. Shackleton, 1987). Moreover, although permanent Northern Hemisphere glaciation did not begin until 2.7 Ma (Haug et al., 2005), the ice-raftered debris (IRD) of deep-sea sediments in the Atlantic Ocean suggests a significant increase of sea ice since about 7–5 Ma (Jansen and Sjøholm, 1991; Larsen et al., 1994). Even if such early IRD records were not from

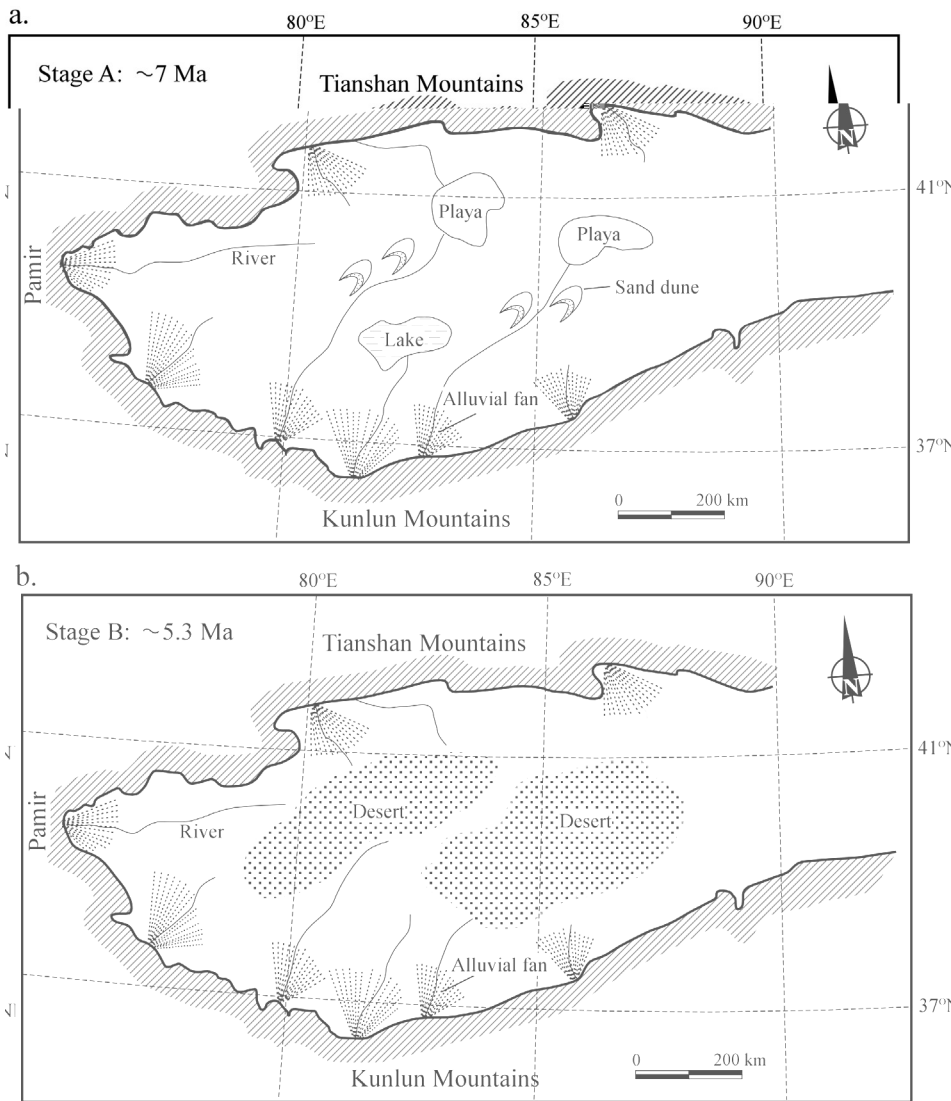


Fig. 7. Schematic maps show that sparsely distributed sand dunes together with diverse environments (e.g., river, lake, playa) at ~ 7 Ma (a), whereas large dune field occurred in the Tarim Basin since ~ 5.3 Ma (b).

land-based ice sheet in the high latitude northern hemisphere, the ice-rafting history of sea ice reflected the onset of remarkable climatic cooling in the northern hemisphere at least since the latest Miocene (Fig. 8c). The significantly enlarged polar ice volumes resulted in the rapid declining of global eustatic sea level since 5.3 Ma (Haq et al., 1987; Fig. 8d).

Additionally, the Asian interior is far from oceans. The prevailing westerlies bring limited water vapors from the Atlantic Ocean to the studied region (Fig. 9). By the end of the Eocene (after 34 million years ago), the Paratethys Ocean was separated from the Neotethys Ocean and experienced stepwise retreat (Rögl, 1999). From the Pliocene epoch onward (after 5 Ma), the former Paratethys Ocean has been progressively shallower and shrinking, splitting into a couple of inland seas (Popov et al., 2004; Olteanu and Jipa, 2006). At present, only the Black Sea, Caspian Sea and Aral Sea remain of what was once a vast inland sea (Fig. 9). In this context, the Paratethys Ocean experienced rapid retreat since the end of the Miocene, this would reduce eastward water vapor transport by westerlies leading to the intensified aridity since 5.3 Ma in the region studied. Moreover, the decrease in sea surface temperature during this time interval decreased sea water evaporation, this would also reduce moisture transportation to the Asian interior.

It is important to stress that except the global scale climatic event, regional effects related to active mountain building should be also considered. Firstly, significant crustal shortening and tectonic uplifts of high mountains surrounding the two studied basins occurred ca. 7–5 Ma (e.g. Métivier et al., 1998; Zheng et al., 2000; Hubert-Ferrari et al., 2007; Sun et al., 2008, 2009b; Sun and Zhang, 2009), therefore, the increasing rain shadow effect of the uplifted mountains might also result in the enhanced aridity and consequently the stable carbon isotope shift since the latest Miocene. Secondly, in addition to the effect of global cooling on the global eustatic sea level change and thus the retreat of the Paratethys Ocean, the collisions of Indian, African, and Arabian plates with the Eurasia during the Cenozoic also contributed greatly to the westward retreat of the Paratethys Ocean (Rögl, 1999; Popov et al., 2004). Therefore, both climatic and regional tectonic factors have influenced the aridity in the western inland basins of China since the latest Miocene.

7. Conclusion

We reconstruct long-term $\delta^{13}\text{C}$ variations of organic matter during the late Cenozoic in the Tarim and Junggar Basins, which are located in the Asian interior. Both records indicate that stable

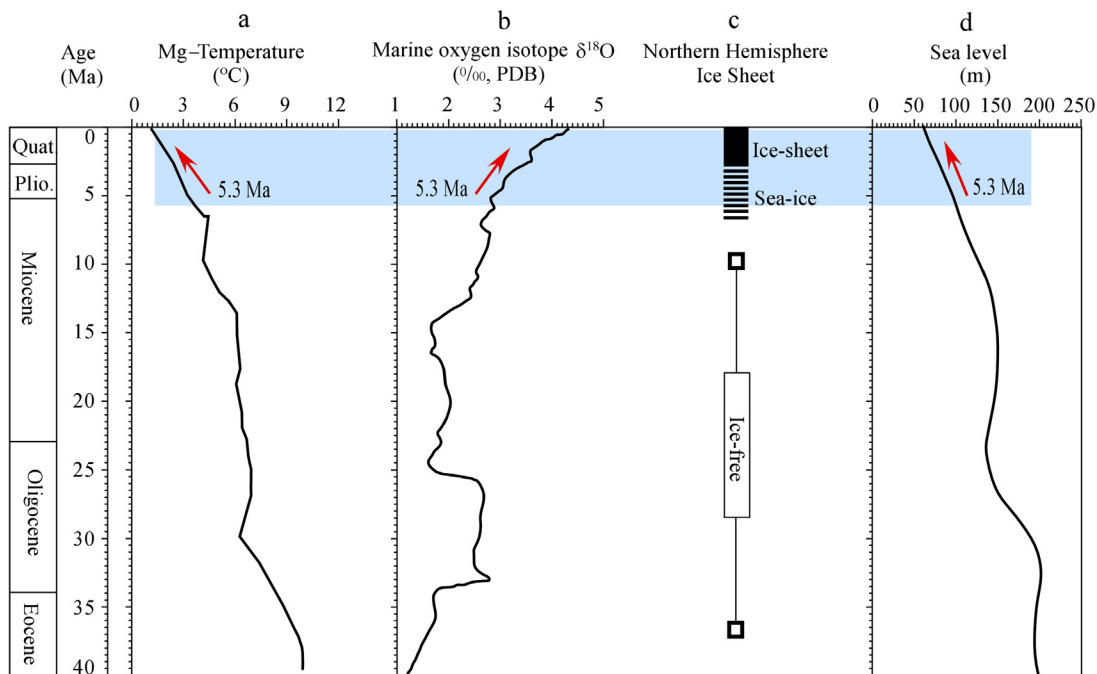


Fig. 8. Correlations among the Mg/Ca derived temperature records (a) (Lear et al., 2000), the composite oxygen isotope curve (b) (Zachos et al., 2001), the ice sheet record in the northern hemisphere (c), after (Zachos et al., 2001), and the sea level fluctuations (d) (Haq et al., 1987).

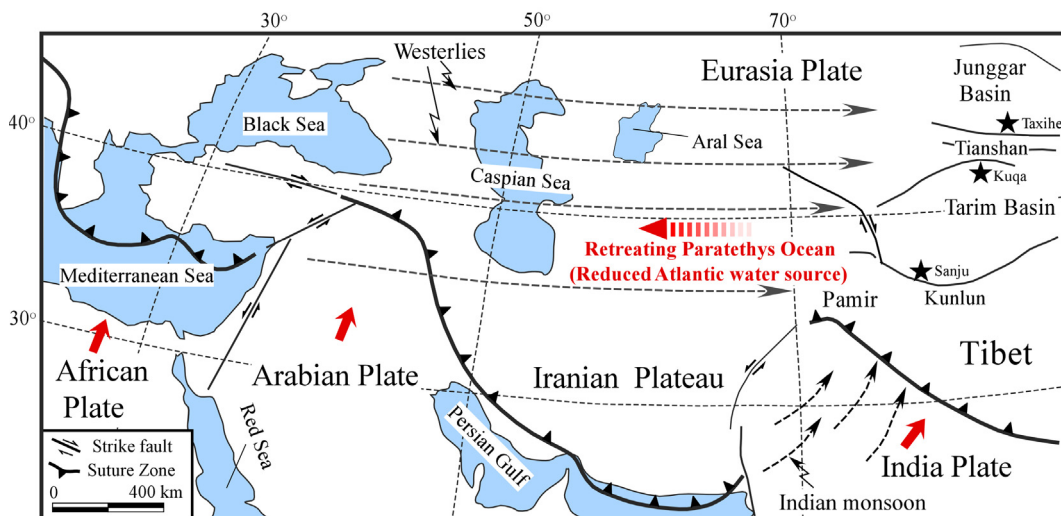


Fig. 9. Map shows wind patterns in the Asian interior. The Indian monsoon is blocked by the Tibetan Plateau, while the main moisture source in the studied region is transported by Westerlies from the Atlantic Ocean. The shrink of the Paratethys Ocean during the late Cenozoic in response to both climatic cooling induced global eustatic sea level decline and the collision of Indian, Arabian, and African plates with Eurasia would reduce the eastward water vapor transfer to the Asian interior. Black stars indicate the locations of sections mentioned in the text. The red arrows indicate the moving directions of the Indian, Arabian, and African plates. (For interpretation of the references to color in this figure legend, the reader is referred to the web version of this article.)

carbon isotopic compositions shifted towards higher values at 5.3 Ma, reflecting a regional-scale ecological change. This ecological shift is simultaneous with regional aridity indicated by multiple climatic proxies. Therefore, we attribute this late Miocene/early Pliocene vegetation shift marked by either C₄ expansion or shifts in C₃ species to the enhanced aridity rather than decreased atmospheric pCO₂. The dramatic retreat of the Paratethys Ocean, in response to decreased global eustatic sea level and the tectonic collision of Indian, Arabian, and African plates with Eurasia, resulted in the regional aridity in the Asian interior by reducing eastward moisture transportation. The strengthening rain shadow effects, related to the active uplift of the surrounding mountains (e.g. Kunlun and Tianshan mountains), might also con-

trolled the regional aridity and ecological shift since the end of Miocene.

Acknowledgements

This work was supported by the National Basic Research Program of China (973 Program) (2013CB956400), the “Strategic Priority Research Program” of the Chinese Academy of Sciences (XDB03020500), and the National Nature Science Foundation of China (grants 41290251 and 41272203). We thank Zhiyong Zhang, Liqiang Xie, and Fei Tan for helps in field sampling. We are grateful to Dr. David L. Fox, and an anonymous reviewer for their detailed and thoughtful reviews that improved the manuscript greatly.

Appendix A. Supplementary material

Supplementary material related to this article can be found online at <http://dx.doi.org/10.1016/j.epsl.2013.08.027>.

References

- Aouac, J.P., Tapponnier, P., 1993. Kinematic model of active deformation in central Asia. *Geophys. Res. Lett.* 20, 895–898.
- Behrensmeyer, A.K., Quade, J., Cerling, T.E., Kappelman, J., Khan, I.A., Copeland, P., Roe, L., Hicks, J., Stubblefield, P., Willis, B.J., Latorre, C., 2007. The structure and rate of late Miocene expansion of C_4 plants: Evidence from lateral variation in stable isotopes in paleosols of the Siwalik Group, northern Pakistan. *Geol. Soc. Am. Bull.* 119, 1486–1505.
- Biasatti, D., Wang, Y., Deng, T., 2010. Strengthening of the East Asian summer monsoon revealed by a shift in seasonal patterns in diet and climate after 2–3 Ma in northwest China. *Palaeogeogr. Palaeoclimatol. Palaeoecol.* 297, 12–25.
- Bywater-Reyes, S., Carrapa, B., Clementz, M., Schoenbohm, L., 2010. Effect of late Cenozoic aridification on sedimentation in the Eastern Cordillera of northwest Argentina (Angastaco basin). *Geology* 38, 235–238.
- Cande, S.C., Kent, D.V., 1995. Revised calibration of the geomagnetic polarity timescale for the Late Cretaceous and Cenozoic. *J. Geophys. Res.* 100, 6093–6095.
- Cerling, T.E., Quade, J., Wang, Y., Bowman, J.R., 1989. Carbon isotopes in soils and paleosols as ecological and paleoecologic indicators. *Nature* 341, 138–139.
- Cerling, T.E., Wang, Y., Quade, J., 1993. Expansion of C_4 ecosystems as an indicator of global ecological change in the late Miocene. *Nature* 361, 344–345.
- Cerling, T.E., Harris, B., MacFadden, M., Leakey, J., Quade, V., Elsenmann, J., Ehleringer, J.R., 1997. Global vegetation change through the Miocene/Pliocene boundary. *Nature* 389, 153–158.
- Charreau, J., Kent-Corson, M.L., Barrier, L., Augier, R., Ritts, B.D., Chen, Y., France-Lannord, C., Guillette, C., 2012. A high-resolution stable isotopic record from the Junggar Basin (NW China): Implications for the paleotopographic evolution of the Tianshan Mountains. *Earth Planet. Sci. Lett.* 341/344, 158–169.
- Dean, W.E., Schwab, A., 2000. Holocene environmental and climatic change in the Northern Great Plains as recorded in the geochemistry of sediments in Pickerel Lake, South Dakota. *Quat. Int.* 67, 5–20.
- Dettman, D.L., Kohn, M.J., Quade, J., Ryerson, F.J., Ojha, T.P., Hamidullah, S., 2001. Seasonal stable isotope evidence for a strong Asian monsoon throughout the past 10.7 m.y. *Geology* 29, 31–34.
- Diefendorf, A.F., Mueller, K.E., Wing, S.L., Kochd, P.L., Freeman, K.H., 2010. Global patterns in leaf ^{13}C discrimination and implications for studies of past and future climate. *Proc. Natl. Acad. Sci. USA* 107, 5738–5743.
- Ding, Z.L., Yang, S.L., 2000. C_3/C_4 vegetation evolution over the last 7.0 Myr in the Chinese Loess Plateau: Evidence from pedogenic carbonate $\delta^{13}\text{C}$. *Palaeogeogr. Palaeoclimatol. Palaeoecol.* 160, 291–299.
- Edwards, G.E., Walker, D.A., 1983. C_3 , C_4 : Mechanisms, and Cellular and Environmental Regulation of Photosynthesis. Blackwell Scientific, Oxford.
- Edwards, E.J., Osborne, C.P., Strömborg, C.A.E., Smith, S.A., 2010. The origins of C_4 grasslands: Integrating evolutionary and ecosystem science. *Science* 328, 587–591.
- Emmerich, W.E., 2007. Ecosystem water use efficiency in a semiarid shrubland and grassland community. *Rangeland Ecol. Manage.* 60, 464–470.
- Fang, X.M., Lü, L.Q., Yang, S.L., Li, J.J., An, Z.S., Jiang, P.A., Chen, X.L., 2002. Loess in Kunlun Mountains and its implications on desert development and Tibetan Plateau uplift in west China. *Sci. China Ser. D* 45, 289–299.
- Farquhar, G.D., Richards, R.A., 1984. Isotopic composition of plant carbon correlates with water-use efficiency of wheat genotypes. *Aust. J. Plant Physiol.* 11, 539–552.
- Fox, D.L., Koch, P.L., 2003. Tertiary history of C_4 biomass in the Great Plains, USA. *Geology* 31, 809–812.
- Fox, D.L., Koch, P.L., 2004. Carbon and oxygen isotopic variability in Neogene Paleosol carbonates: Constraints on the evolution of the C_4 -grasslands of the Great Plains, USA. *Palaeogeogr. Palaeoclimatol. Palaeoecol.* 207, 305–329.
- Fox, D.L., Honey, J.G., Martin, R.A., Peláez-Campomanes, P., 2012a. Pedogenic carbonate stable isotope record of environmental change during the Neogene in the southern Great Plains, southwest Kansas, USA: Carbon isotopes and the evolution of C_4 -dominated grasslands. *Geol. Soc. Am. Bull.* 124, 444–462, <http://dx.doi.org/10.1130/B30401.1>.
- Fox, D.L., Honey, J.G., Martin, R.A., Peláez-Campomanes, P., 2012b. Pedogenic carbonate stable isotope record of environmental change during the Neogene in the southern Great Plains, southwest Kansas, USA: Oxygen isotopes and paleoclimate during the evolution of C_4 -dominated grasslands. *Geol. Soc. Am. Bull.* 124, 431–443, <http://dx.doi.org/10.1130/B30402.1>.
- Haq, B.U., Hardenbol, J., Vail, P.R., 1987. Chronology of fluctuating sea levels since the Triassic (250 million years ago to present). *Science* 235, 1156–1167.
- Haug, G.H., Ganopolski, A., Sigman, D.M., Rosell-Mele, A., Swann, G.E.A., Tiedemann, R., Jaccard, S.L., Bollmann, J., Maslin, M.A., Leng, M.J., Eglington, G., 2005. North Pacific seasonality and the glaciation of North America 2.7 million years ago. *Nature* 433, 821–825.
- Hopley, P.J., Marshall, J.D., Weedon, G.P., Latham, A.G., Herries, A.I.R., Kuykendall, K.L., 2007. Orbital forcing and the spread of C_4 grasses in the late Neogene: Stable isotope evidence from South African speleothems. *J. Hum. Evol.* 53, 620–634.
- Huang, Y., Clemens, S.C., Liu, W., Wang, Y., Prell, W.L., 2007. Large-scale hydrological change drove the late Miocene C_4 plant expansion in the Himalayan foreland and Arabian Peninsula. *Geology* 35, 531–534.
- Hubert-Ferrari, A., Suppe, J., Gonzalez-Mieres, R., Wang, X., 2007. Mechanisms of active folding of the landscape (southern Tian Shan, China). *J. Geophys. Res.* 112, B03S09, <http://dx.doi.org/10.1029/2006JB004362>.
- Jacobs, B., Kingston, J.D., Jacobs, L., 1999. The origin of grass-dominated ecosystems. *Ann. Mo. Bot. Gard.* 399, 673–676.
- Jansen, E., Sjøholm, J., 1991. Reconstruction of glaciation over the past 6 Myr from ice-borne deposits in the Norwegian Sea. *Nature* 349, 600–603.
- Jia, C., 1997. Structural Geology and Petroleum Potential in the Tarim Basin, China. Pet. Ind. Press House, Beijing.
- Jia, G.D., Ping, P.A., Zhao, Q.H., Jian, Z.M., 2003. Changes in terrestrial ecosystem since 30 Ma in East Asia: Stable isotope evidence from black carbon in the South China Sea. *Geology* 31, 1093–1096.
- Kennett, J.P., 1977. Cenozoic evolution of Antarctic glaciation, the circum-Antarctic Ocean, and their impact on global paleoceanography. *J. Geophys. Res.* 82, 3843–3859.
- Kohn, M.J., 2010. Carbon isotope compositions of terrestrial C_3 plants as indicators of (paleo)ecology and (paleo)climate. *Proc. Natl. Acad. Sci. USA* 107, 19691–19695.
- Kohn, M.J., Fremd, T.J., 2008. Miocene tectonics and climate forcing of biodiversity, western United States. *Geology* 36, 783–786.
- Larsen, H.C., Saunders, A.D., Clift, P.D., Beget, J., Wei, W., Spezzaferri, S., 1994. Seven million years of glaciation in Greenland. *Science* 264, 952–955.
- Last, W.M., 1990. Paleochemistry and paleohydrology of Ceylon Lake, a salt-dominated playa basin in the Northern Great Plains, Canada. *J. Paleol.* 4, 219–238.
- Last, W.M., Vance, R.E., 2002. The Holocene history of Oro Lake, one of the western Canada's longest continuous lacustrine records. *Sediment. Geol.* 148, 161–184.
- Latorre, C., Quade, J., McIntosh, W.C., 1997. The expansion of C_4 grasses and global change in the late Miocene: Stable isotope evidence from the Americas. *Earth Planet. Sci. Lett.* 146, 83–96.
- Lear, C.H., Elderfield, H., Wilson, P.A., 2000. Cenozoic deep-sea temperatures and global ice volumes from Mg/Ca in benthic foraminiferal calcite. *Science* 287, 269–272.
- Li, D., Liang, D., Jia, C., Wang, G., Wu, Q., He, D., 1996. Hydrocarbon accumulations in the Tarim Basin, China. *Am. Assoc. Pet. Geol. Bull.* 80, 1587–1603.
- Liu, W.G., Li, X.Z., An, Z.S., Xu, L.M., 2013. Total organic carbon isotopes: A novel proxy of lake level from Lake Qinghai in the Qinghai-Tibet Plateau, China. *Chem. Geol.* 347, 153–160.
- Long, S., 1999. Environmental responses. In: Sage, R.F., Monson, R.K. (Eds.), C_4 Plant Biology. Academic Press, San Diego, pp. 215–249.
- Martin, R.A., Peláez-Campomanes, P., Honey, J.G., Fox, D.L., Zakrzewski, R.J., Albright, L.B., Lindsay, E.H., Opdyke, N.D., Goodwin, H.T., 2008. Rodent community change at the Pliocene-Pleistocene transition in southwestern Kansas and identification of the Microtus immigration event on the Central Great Plains. *Palaeoecol. Palaeoclimatol. Palaeoecol.* 267, 196–207.
- Métivier, F., Gaudemer, Y., Tapponnier, P., Meyer, B., 1998. Northeastward growth of the Tibet plateau deduced from balanced reconstruction of two depositional areas: The Qaidam and Hexi Corridor basins, China. *Tectonics* 17, 823–842.
- Meyers, P.A., 1992. Changes in organic carbon stable isotope ratios across the K/T boundary: Global or local control? *Chem. Geol.* 101, 283–291.
- Meyers, P.A., Horie, S., 1993. An organic carbon isotopic record of glacial–postglacial change in atmospheric $p\text{CO}_2$ in the sediments of Lake Biwa, Japan. *Palaeogeogr. Palaeoclimatol. Palaeoecol.* 105, 171–178.
- Miller, K.G., Wright, J.D., Fairbanks, R.G., 1991. Unlocking the ice house: Oligocene–Miocene oxygen isotopes, eustasy, and margin erosion. *J. Geophys. Res.* 96, 6829–6848.
- Molnar, P., Tapponnier, P., 1975. Cenozoic tectonics of Asia: Effects of a continental collision. *Science* 189, 419–426.
- O'Leary, M.H., 1981. Carbon isotope fractionation in plants. *Phytochemistry* 20, 553–567.
- O'Leary, M.H., 1988. Carbon isotopes in photosynthesis. *Bioscience* 38, 328–336.
- Olteanu, R., Jipa, D.C., 2006. Dacian Basin environmental evolution during upper Neogene within the Paratethys domain. *Geo-Eco-Mar.* 12, 91–105.
- Osborne, C.P., Beerling, D.J., 2006. Nature's green revolution: The remarkable evolutionary rise of C_4 plants. *Philos. Trans. R. Soc. Lond. B, Contain. Pap. Biol. Character* 361, 173–194.
- Osmond, C.B., Winter, K., Ziegler, H., 1982. Functional significance of different pathways of CO_2 fixation in photosynthesis. In: Lange, O.L., Noble, P.S., Osmond, C.B., Ziegler, H. (Eds.), Encyclopedia of Plant Physiology, New Series, vol. 12B. Springer-Verlag, Berlin, pp. 479–547.
- Pagani, M., Freeman, K.H., Arthur, M.A., 1999. Late Miocene CO_2 concentrations and the expansion of C_4 grasses. *Science* 285, 876–879.
- Pagani, M., Zachos, J.C., Freeman, K.H., Tipple, B., Bohaty, S., 2005. Marked decline in atmospheric carbon dioxide concentrations during the Paleogene. *Science* 309, 600–603.

- Pagani, M., Caldeira, K., Berner, R., Beerling, D.J., 2009. The role of terrestrial plants in limiting atmospheric CO₂ decline over the past 24 million years. *Nature* 460, 85–89.
- Pearson, P.N., Palmer, M.R., 1999. Middle Eocene seawater pH and atmospheric carbon dioxide concentrations. *Science* 284, 824–826.
- Popov, S.V., Rögl, F., Rozanov, A.Y., Steininger, Fritz F., Shcherba, I.G., Kovac, M., 2004. Lithological-paleogeographic maps of Paratethys. CSF, Cour. Forsch.inst. Senckenb., vol. 250, pp. 1–46.
- Quade, J., Cerling, T.E., Bowman, J.R., 1989. Development of Asian monsoon revealed by marked ecological shift during the latest Miocene in northern Pakistan. *Nature* 342, 163–166.
- Raven, P.H., Event, R.F., Eichhorn, S.E., 1999. *Biology of Plants*, 6th ed. W.H. Freeman Co., New York.
- Read, J.J., Johnson, D.A., Asay, K.H., Tieszen, L.T., 1991. Carbon isotope discrimination, gas exchange, and water-use efficiency in Crested Wheatgrass clones. *Crop Sci.* 31, 1203–1208.
- Read, J.J., Johnson, D.A., Asay, K.H., Tieszen, L.T., 1992. Carbon isotope discrimination: Relationship to yield, gas exchange and water-use efficiency in field grown Crested Wheatgrass. *Crop Sci.* 32, 168–175.
- Retallack, G.J., 1998. Grassland ecosystems as a biological force in dusty dry regions. In: Busacca, A.J. (Ed.), *Dust, Aerosols, Loess Soils and Global Change*, vol. 190. Washington State Univ. Coll. Agric. Home Econ. Misc. Publ., pp. 171–174.
- Retallack, G.J., 2001. Cenozoic Expansion of Grasslands and Climatic Cooling. *J. Geol.* 109, 407–426.
- Rögl, F., 1999. Mediterranean and Paratethys. Facts and hypotheses of an Oligocene to Miocene paleogeography (short overview). *Geol. Carpath.* 50, 339–349.
- Schütt, B., 2000. Holocene paleohydrology of playa-lake systems in central Spain: A reconstruction based on mineral composition of the lacustrine sediments. *Quat. Int.* 73/74, 7–27.
- Shackleton, N.J., 1987. Oxygen isotopes, ice volume and sea level. *Quat. Sci. Rev.* 6, 183–190.
- Sinha, R., Raymahashay, B.C., 2004. Evaporite mineralogy and geochemical evolution of the Sambhar Salt Lake, Thar Desert, Rajasthan, India. *Sediment. Geol.* 166, 59–71.
- Stevenson, B.A., Kelly, E.F., McDonald, E.V., Busacca, A.J., 2005. The stable carbon isotope composition of soil organic carbon and pedogenic carbonates along a bioclimatic gradient in the Palouse region, Washington State, USA. *Geoderma* 124, 37–47.
- Still, C.J., Berry, J.A., Ribas-Carbo, M., Helliker, B.R., 2003. The contribution of C₃ and C₄ plants to the carbon cycle of a tallgrass prairie: An isotopic approach. *Oecologia* 136, 347–359.
- Su, P.X., Xie, T.T., Zhou, Z.J., 2011. Geographic distribution of C₄ plant species in desert regions of China and its relation with climate factors. *J. Desert Res.* 31, 267–276.
- Sun, J.M., Liu, T.S., 2006. The age of the Taklimakan Desert. *Science* 312, 1621.
- Sun, J.M., Zhang, Z.Q., 2008. Palynological evidence for the Mid-Miocene Climatic Optimum recorded in Cenozoic sediments of the Tian Shan Range, northwestern China. *Glob. Planet. Change* 64, 53–68.
- Sun, J.M., Zhang, Z.Q., 2009. Syntectonic growth strata and implications for late Cenozoic tectonic uplift in the northern Tian Shan, China. *Tectonophysics* 463, 60–68.
- Sun, J.M., Zhang, L.Y., Deng, C.L., Zhu, R.X., 2008. Evidence for enhanced aridity in the Tarim Basin of China since 5.3 Ma. *Quat. Sci. Rev.* 27, 1012–1023.
- Sun, J.M., Zhang, Z.Q., Zhang, L.Y., 2009a. New evidence on the age of the Taklimakan Desert. *Geology* 37, 159–162.
- Sun, J.M., Li, Y., Zhang, Z.Q., Fu, B.H., 2009b. Magneostriatigraphic data on the Neogene growth folding in the foreland basin of the southern Tianshan Mountains. *Geology* 37, 1051–1054.
- Sun, D.H., Bloemendal, J., Yi, Z.Y., Zhu, Y.H., Wang, X., Zhang, Y.B., Li, Z.J., Wang, F., Han, F., Zhang, Y., 2011. Palaeomagnetic and palaeoenvironmental study of two parallel sections of late Cenozoic strata in the central Taklimakan Desert: Implications for the desertification of the Tarim Basin. *Palaeogeogr. Palaeoclimatol. Palaeoecol.* 300, 1–10.
- Tada, R., Zheng, H.B., Isozaki, Y., Hasegawa, H., Sun, Y.B., Yang, W.G., Wang, K., Toyoda, S., 2010. Desertification and dust emission history of the Tarim Basin and its relation to the uplift of northern Tibet. *Geol. Soc. London Spec. Publ.* 342, 45–65.
- Tipple, B.J., Pagani, M., 2010. A 35 Myr North American leaf-wax compound-specific carbon and hydrogen isotope record: Implications for C₄ grasslands and hydrologic cycle dynamics. *Earth Planet. Sci. Lett.* 299, 250–262.
- Tipple, B.J., Meyers, S.R., Pagani, M., 2010. Carbon isotope ratio of Cenozoic CO₂: A comparative evaluation of available geochemical proxies. *Paleceanography* 25, <http://dx.doi.org/10.1029/2009PA001851>. PA3202.
- Urban, M.A., Nelson, D.M., Jiménez-Moreno, G., Châteauneuf, J., Pearson, A., Hu, F.S., 2010. Isotopic evidence of C₄ grasses in southwestern Europe during the Early Oligocene–Middle Miocene. *Geology* 38, 1091–1094.
- Wang, Y., Deng, T., 2005. A 25 m.y. isotopic record of paleodiet and environmental change from fossil mammals and paleosols from the NE margin of the Tibetan Plateau. *Earth Planet. Sci. Lett.* 236, 322–338.
- Wang, Y., Deng, T., Biasatti, D., 2006. Ancient diets indicate significant uplift of southern Tibet after ca. 7 Ma. *Geology* 34, 309–312.
- Wang, Y., Deng, T., Flynn, L., Wang, X., An, Y., Xu, Y., Parker, W., Lochner, E., Zhang, C., Biasatti, D., 2012. Late Neogene environmental changes in the central Himalaya related to tectonic uplift and orbital forcing. *J. Asian Earth Sci.* 44, 62–76.
- Wasson, R.J., Smith, G.I., Agrawal, D.P., 1984. Late Quaternary sediments, minerals, and inferred geochemical history of Didwana lake, Thar Desert, India. *Palaeogeogr. Palaeoclimatol. Palaeoecol.* 46, 345–372.
- Zachos, J., Pagani, M., Sloan, L., Thomas, E., Billups, K., 2001. Trends, rhythms, and aberrations in global climate 65 Ma to present. *Science* 292, 686–693.
- Zhang, Z.Q., Sun, J.M., 2011. Palynological evidence for Neogene environmental change in the foreland basin of the southern Tianshan range, northwestern China. *Glob. Planet. Change* 75, 56–66.
- Zhang, C.F., Wang, Y., Deng, T., Wang, X.M., Biasatti, D., Xu, Y.F., Li, Q., 2009. C₄ expansion in the central Inner Mongolia during the latest Miocene and early Pliocene. *Earth Planet. Sci. Lett.* 287, 311–319.
- Zhang, C.F., Wang, Y., Li, Q., Wang, X.M., Deng, T., Tseng, Z.J., Takeuchi, G.T., Xie, G.P., Xu, Y.F., 2012. Diets and environments of late Cenozoic mammals in the Qaidam Basin, Tibetan Plateau: Evidence from stable isotopes. *Earth Planet. Sci. Lett.* 333/334, 70–82.
- Zheng, H.B., Powell, C.M., An, Z.S., Zhou, J., Dong, G.R., 2000. Pliocene uplift of the northern Tibetan Plateau. *Geology* 28, 715–718.
- Zheng, H.B., Chen, H.Z., Cao, J.J., 2002. Paleoenvironmental significance of the Pliocene–early Pleistocene eolian loess in the southern Tarim Basin. *Chin. Sci. Bull.* 47, 226–230.
- Zheng, H.B., Powell, C., Butcher, K., Cao, J.J., 2003. Late Neogene aeolian loess deposition in southern Tarim Basin and its palaeoenvironmental significance. *Tectonophysics* 375, 49–59.
- Zheng, H.B., Tada, R., Jia, J.T., Lawrence, C., Wang, K., 2010. Cenozoic sediments in the southern Tarim Basin: Implications for the uplift of northern Tibet and evolution of the Taklimakan Desert. *Geol. Soc. London Spec. Publ.* 342, 67–78.
- Zhu, Z.D., Wu, Z., Liu, S., Di, X.M., 1980. *An Outline on Chinese Deserts*. Science Press, Beijing.